Korean J. Chem. Eng., **21**(5), 929-934 (2004)

Effects of Process Parameters for the Preparation of C/SiC Composites in the F-Chemical Vapor Infiltration Reactor

Hee Kim, Gui-Yung Chung†, Hyung-Hoi Koo* and Woon-Hyung Baek*

Dept. of Chemical Engineering, Hong-Ik University, 72-1 Sangsu-dong, Mapo-ku, Seoul 121-791, Korea
*ADD, Yuseong P.O. Box 35-5, Daejeon 305-600, Korea
(*Received 8 February 2004 • accepted 2 July 2004*)

Abstract–Mathematical modeling for the preparation of C/SiC composites from methyl-trichlorosilane in a F-CVI (Forced-chemical vapor infiltration) reactor was studied. Changes of pressure, concentration and porosity with time were predicted by the modeling. Pressure in the preform decreased sharply along the direction of gas flow. Pore entrances were plugged at 130 min reaction time in the conditions of this research. As pore entrances became plugged, the pressure at the pore entrance increased rapidly. The time when the preform should be overturned in the middle of deposition process for a uniform deposition could be decided by observing the radius of pore entrance. At the gas outlet of the preform, MTS was depleted completely and the fraction of HCl, i.e., the undesirable byproduct, became 0.42.

Key words: C/SiC Composites, F-CVI, Process Parameters, Mathematical Modeling

INTRODUCTION

Ceramic composite materials have been drawing considerable attention in the several industrial fields recently. This is because composite materials compensate for shortcomings of each ceramic component. Hence, good properties of every ingredients can be used. For example, carbon materials are suitable for high temperature structural materials because of their good mechanical properties such as hardness and wear resistance. They are also light and not corrosive. However, their utilization has been limited because they are easily breakable. These shortcomings can be improved by reinforcing with fibers and making composite materials by Chemical Vapor Infiltration (CVI). Fibers absorb energy when ceramic composites are elongated and broken.

CVI was originated in efforts to densify porous graphite bodies by infiltration of carbon [Delhaes, 2002]. The earliest report of the use of CVI was a patent for infiltrating fibrous alumina with chromium carbides [Jenkin, 1964]. Since then this technique has been developed commercially such that half of the carbon-carbon composites currently produced are made by CVI [Bickerdike et al., 1992]. In the method of CVI, the precursor gas diffuses into a porous preform and reacts at pore walls, which leads to deposition of matrix materials [Zhang et al., 2002]. The ideal result would be a dense composite. It can produce large pieces of composite materials with complex shape.

Many different types of CVI reactor have been developed. They are the isothermal CVI (I-CVI), the temperature gradient CVI (TG-CVI), the isothermal forced-flow CVI (F-CVI), the pressure-pulsed CVI technique (P-CVI). In this research, F-CVI has been studied.

Manufacturing and modeling of fiber-reinforced ceramic composites by CVI were studied by many researchers [Birakayala and Evans, 2002; Luo, 2002; Nannetti et al., 2002]. Ceramic composites reinforced with fiber bundles were studied by Rossignol et al. [1984] and Tai and Chou [1989]. Those reinforced with short fibers were studied by Gupte [1989], Starr [1987], and Jensen [1989]. Manufacturing ceramic composites reinforced with multilayer woven fabrics and its mathematical modeling were studied by Chung et al. [1991, 1992, 1993] and Kim et al. [1996]. Three void regions in the preform were considered: holes between tows, gaps around fibers, and spaces between plies. Reactant gases diffuse into three void regions and react to produce solid deposits. Jin et al. [1999, 2000] modeled CVI assuming fiber surfaces as an evolving interface. Numerical simulations were used to optimize parameters of CVI processes [Li et al., 2003; Jiang et al., 2002]. An overall deposition reaction which is the first order on the reactant concentration and the surface area available for deposition was assumed [Chung et al., 1993; Lee, 2002].

Diffusion of reactant gases from the outside surface of a preform results in a concentration gradient, a nonuniform deposition profile. and, as a result, an occlusion of the outer surface of the preform before filling the interior voids completely [Chung et al., 1991, 1992, 1993; Cho, 1996].

The objective of this work was modeling the preparation of fiber-reinforced SiC/C composites by F-CVI of SiC from methyltrichlorosilane (MTS) and H_2. Effects of parameters of infiltration reaction could be predicted by mathematical modeling. Time changes of pore size, porosity, amount of deposition, and pressure gradient, etc. were estimated.

MODEL DEVELOPMENT

The system is a cylindrical preform that is composed of layers of carbon fiber bundle. However, spaces between layers and holes between tows in the preform are ignored. Fibers are nonporous. Pores among fibers are assumed to be distributed evenly in the whole preform. A schematic diagram of the system is shown in Fig. 1. Tortuosity of pores was taken as a square of porosity.

Reactant gases of H_2 and MTS flow from one side to other side of the preform by a forced convection flow in the isothermal reactor

†To whom correspondence should be addressed.
E-mail: gychung@hongik.ac.kr

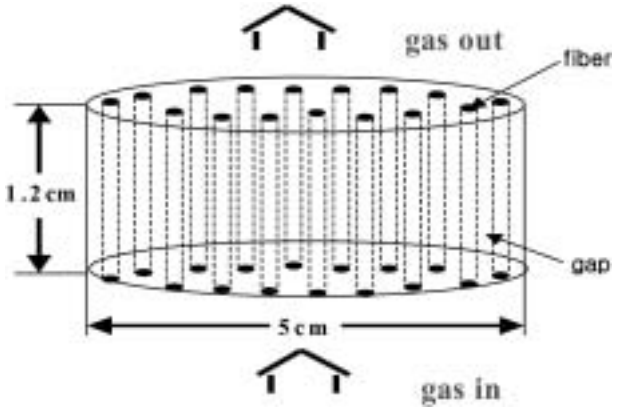

Fig. 1. Schematic diagram of the preform.

(F-CVI). Fractions of gases are functions of z only, the direction of gas flow. Deposition reaction occurs at the outside surfaces of cylindrical fibers in the preform. Pseudo-steady state is assumed for the concentration distribution. In other words, the distribution of gas concentration reaches an equilibrium rapidly compared to the change of fiber radius due to deposition. Although the actual infiltration reaction might have several steps, it is supposed in this research that the following overall deposition reaction of SiC is a first order reaction for the concentration of MTS, i.e., 1 mole of MTS changes into 1 mole of SiC and 3 moles of HCl.

$$CH_3SiCl_3 \rightarrow SiC + 3HCl \quad (1)$$

There is only z-directional convection in pores among fibers. Hence, the molar balance of i-component is as follows:

$$\frac{1}{A}\frac{\partial QC_i}{\partial z} - 2n\pi W k r_f C_A = 0 \quad (2)$$

Here, A is the cross-sectional area of the preform, C_i the concentration of i-component such as MTS, H_2, and HCl, C_A the concentration of MTS, W the number of fibers per unit cross-sectional area of the preform, r_f the radius of fiber, k the first order deposition rate constant, n is the stoichiometric coefficient in Eq. (1), where n is a plus value for products and a minus value for reactants. The first term in Eq. (2) is the change of i-component due to a convectional gas flow and the second one is that due to a deposition. The total molar balance is as follows:

$$\frac{1}{A}\frac{\partial QC}{\partial z} - 4\pi W k r_f C_A = 0 \quad (3)$$

The momentum balance equation for packed columns was used for the calculation of pressure distribution [Bird et al., 2002].

$$\frac{P_z - P_{z+\Delta z}}{\Delta z} = 150\left(\frac{\mu Q_z/A}{d_f^2}\right)\frac{(1-\varepsilon_z)^2}{\varepsilon_z^3} + 1.727\times10^{-6}\left(\frac{\rho\left(\frac{Q}{A}\right)^2}{d_f^2}\right)\frac{(1-\varepsilon_z)}{\varepsilon_z^3} \quad (4)$$

Changes of fiber radius with time were calculated with the following equation:

$$\frac{\partial r_{fz}}{\partial t} = \frac{qM_m}{\rho_m} k C_{A,z} \quad (5)$$

Here, q is the mole number of deposited SiC from 1 mole of MTS. M_m and ρ_m are the molecular weight and the density of SiC, respectively. The amount of deposition per unit cross-sectional area of the preform for the thickness of Δz is expressed as follows:

$$D_z = \pi\sum_{z=0}^{L}(r_{fz}^2 - r_{fo}^2)\Delta z W \rho_m \quad (6)$$

The porosity is obtained in a similar way.

$$\varepsilon_z = 1 - \pi r_{fz}^2 W \quad (7)$$

Using dimensionless parameters such as $\sigma(=r_f/r_{fo})$ and $\xi(=z/H)$, equations were changed into dimensionless form and calculated in the finite different method. Calculations were carried out after the z-axis was divided into 20 elements.

Porosity at z, i.e., ε_z, was calculated first and then P_z, C_z, and Q_z were calculated. With these values, mole fractions of all components, x_i's, were calculated. Fiber radius r_f, amount of infiltration D, and average porosity ε_z were calculated. Calculations were terminated at the time when pores were plugged or pressure was more than an appropriate limit value.

RESULTS AND DISCUSSION

Mathematical modeling was carried out with the parameter values listed in Table 1 and the reaction rate constant of 10 cm/min. This value of reaction rate constant was used in the previous papers [Chung et al., 1991, 1992, 1993] Dimensions of the preform were taken from a sample used in the experiment done in our laboratory. With the mathematical modeling, changes of concentration, pressure, porosity, and amount of deposition were estimated.

1. Changes of Pressure

Time changes of pressures at different positions in the preform are in Fig. 2. In the reactor, gas flows from the bottom to the top of the preform (in z'-direction). The curve at z=0 is the pressure change with time at the gas inlet and that at z=H is those at the gas outlet. As in our experimental setting, the pressure at the gas outlet has been fixed as 100 torr. As the deposition reaction goes on, sizes of pores decrease. Hence, pressures at all positions increase with time. Furthermore, the highest concentration of MTS is at the gas inlet (z=0), and, as a result, the fastest deposition rate is obtained there. Hence, the pressure at the gas inlet increases sharply.

Table 1. Dimensions of the sample and deposition conditions

Deposition temperature	1,273 K
Pressure at the exit	100 torr
Preform : Diameter	5 cm
Thickness	1.2 cm
Initial porosity	0.617
Number of layers	12
Side length of a hole	3.3×10^{-3} cm
Thickness of one layer	0.588 mm
Number of fibers in a bundle	3,000
Diameter of a fiber	7 μm

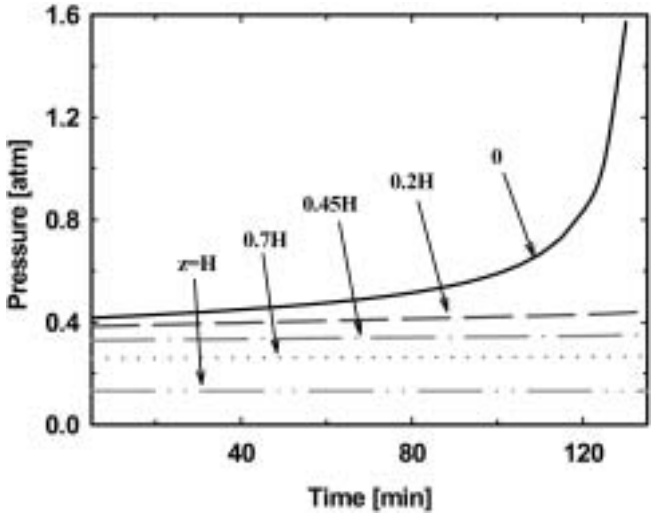

Fig. 2. Changes of pressures at different positions in the preform with time. H means the thickness of the preform. z=0 means the gas inlet and z=H means the gas outlet.

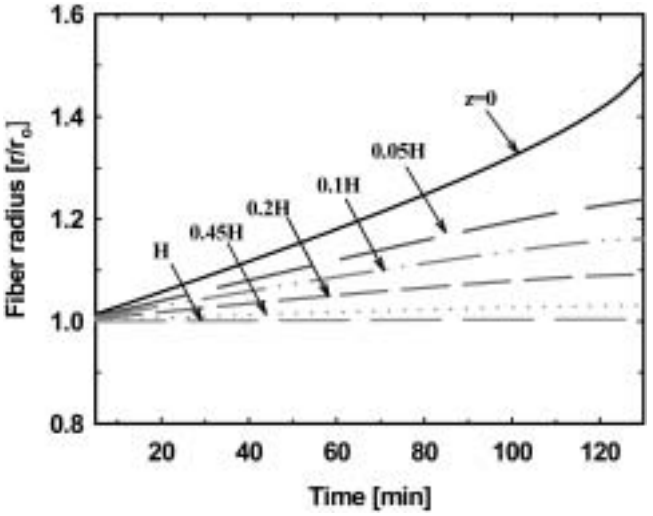

Fig. 4. Changes of the fiber radii with time at different positions in the preform. z=0 means the gas inlet and z=H means the gas outlet.

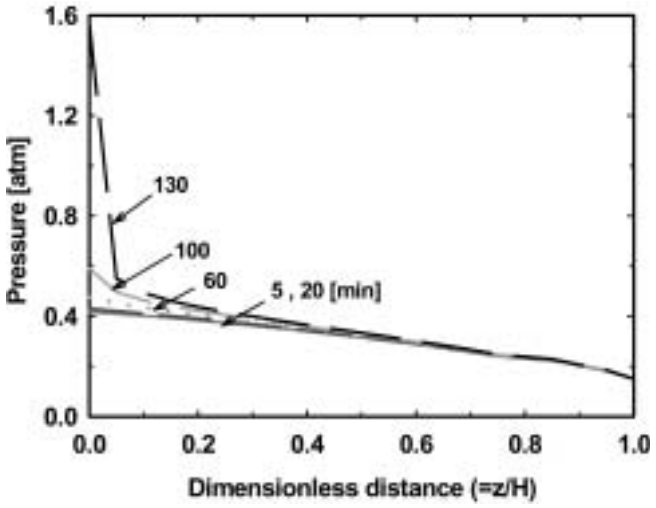

Fig. 3. Distributions of pressure along the direction of gas flow in the preform at different reaction times.

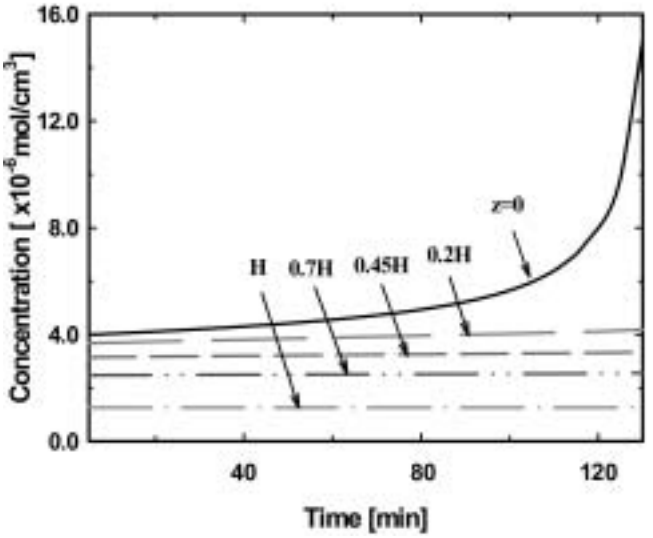

Fig. 5. The concentration of the total gas vs. time at different positions in the preform.

Pressure distributions along the direction of gas flow at different times are in Fig. 3. At the initial stages of process, pressure decreases slowly from the bottom to the top of the preform. However, after 60 min of reaction time, the pressure around the gas inlet increases rapidly. Nevertheless, changes of pressures above z=0.2H of the preform are slight at all reaction times.

Fig. 4 is the time changes of fiber radius at different positions in the preform. As time goes on, fiber radius increases gradually at almost all parts of the preform. As expected, changes of fiber radius around the gas entrance (z=0) are big. At the upper half of the preform (z=0.45H~H), the radii of fibers change very slowly. It is almost the same as changes of pressures above z=0.2H are very small in Fig. 2. The slopes of curves are rather decreasing after 80 min due to plugging of the gas entrance.

2. Changes of the Concentration

Fig. 5 is the time changes of the total concentration of gases at different positions in the preform. Since the ideal gas law has been applied, the total concentration changes in a similar way as pressures do in Fig. 2. There is no big change of total concentration with time above z=0.2H of the preform, but that at the gas inlet changes considerably as pore entrances at z=0 become plugged after 80 min.

Changes of the mole fraction of each component with time in the middle of the preform are in Fig. 6. As the infiltration process goes on, the surface area around fibers becomes large. Hence, the deposition rate increases with the increasing surface area. As a result, the mole fraction of MTS decreases with time, as shown in Fig. 6.

According to the deposition reaction Eq. (1), when one mole of MTS reacts, three moles of HCl are produced and the total mole number of whole gases increases by two moles. Hydrogen would have some role in the deposition reaction. However, according to the reaction Eq. (1), the resultant number of moles of hydrogen does

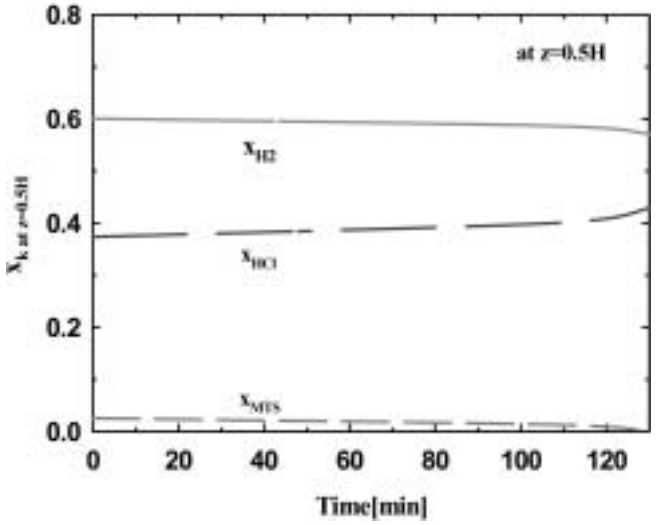

Fig. 6. Changes of the mole fraction of each gas with time in the middle of the preform (at z=0.5H).

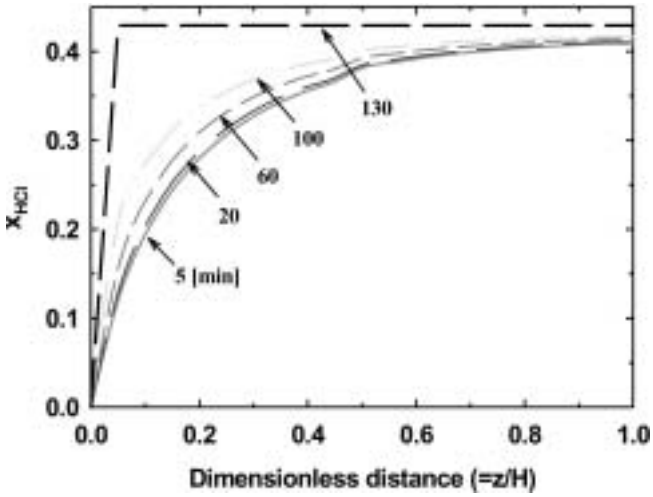

Fig. 8. Distributions of the mole fraction of HCl in the preform at different times.

not change.

In the middle of the preform, the mole fraction of HCl increases with time as that of MTS decreases. As explained above, the mole number of hydrogen does not change and, on the other hand, the mole number of total gases increases with time. Therefore the mole fraction of hydrogen decreases slowly with time.

In Fig. 6, the mole fraction of HCl increases steadily, but, after 110 min, it increases steeply. It is due to plugging of pores at the gas entrance. Since the entrance pressure rises, the pressure in the middle of the preform rises and the rate of deposition becomes faster. So the mole fraction of HCl increases rapidly after 110 min of reaction time.

The distributions of MTS mole fraction in the preform at different times are in Fig. 7. It decreases along the direction of gas flow. Around the gas entrance, the total concentration is high and the reaction rate is fast. So the concentration of MTS decreases quickly and MTS is almost depleted before reaching the gas exit. The mole fraction of MTS becomes 0 at z=0.1H at 130 min of reaction time. It is due to plugging of pores at the gas entrance.

The distributions of HCl mole fraction in the preform at different times are in Fig. 8. As mentioned above, when one mole of MTS is consumed, 3 moles of HCl are produced. Furthermore, as the deposition process goes on, the deposition rate becomes faster due to the increased surface area. Hence, more MTS is consumed and the fraction of HCl increases. When MTS is depleted completely at 130 min as in Fig. 7, the mole fraction of HCl does not change anymore.

3. Changes of Porosity and the Amount of Deposition

Porosities are calculated by using values of fiber radius. Hence, changes of porosity are similar to changes of fiber radius. Fig. 9 is the porosity distributions at different reaction times. The time of plugging pores at the gas entrance is 130 min. At this time, the porosity of the preform at the gas inlet is 0.093 which is theoretically the lowest value. Until 20 min of the reaction time, changes of pres-

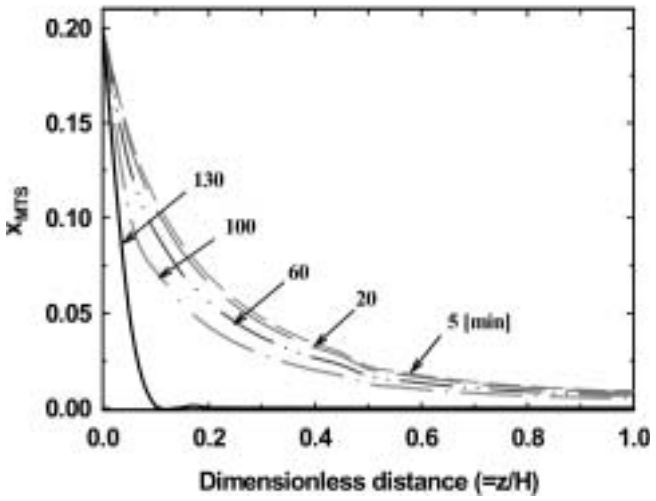

Fig. 7. Distributions of the mole fraction of MTS in the preform at different times.

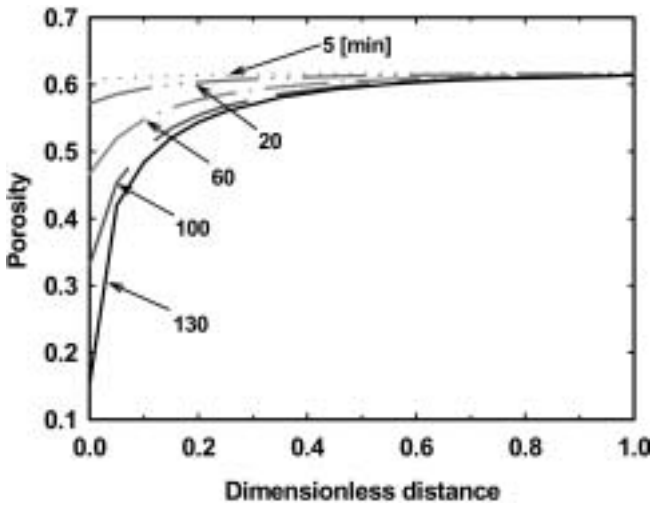

Fig. 9. Distributions of the local porosity in the preform at different times.

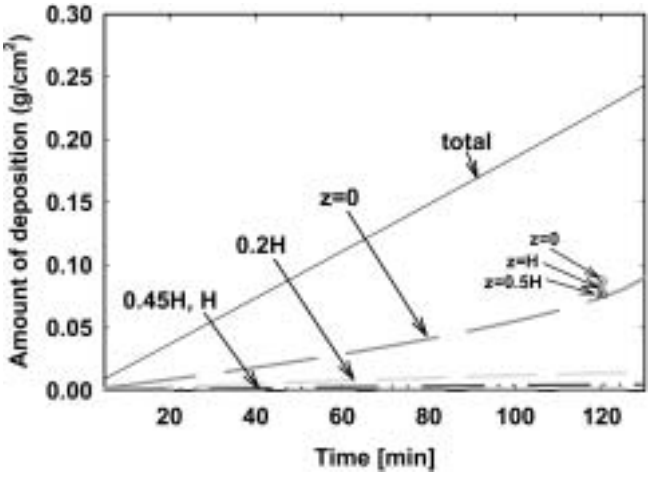

Fig. 10. Changes of the local amount of deposition per unit cross-sectional area of the preform at different positions in the preform. Dotted points are the experimental data [Park et al., 2001].

sure are little as shown in Fig. 3, so porosities in the whole preform are relatively uniform. From this graph, it might be concluded that, in the middle of the deposition reaction, the preform should be overturned at a proper time after 20 min of reaction time to get a uniform deposition through the preform.

Fig. 10 is the amount of deposition vs. time at different positions in the preform. The amount of deposition increases steadily. As the concentration of MTS increases sharply after 100 min at the gas entrance, the amount of deposition increases in a similar way. As pores become plugged, the increasing rate of the amount of deposition decreases.

The experimental data by Park et al. [2001] show a similar value at the entrance of the gas channel. On the contrary, the experimental values at z=0.5H and H are quite more than the calculated values. That was because of a little different structure of the reactor. The exit gas was accumulated at the end of the preform for a while. Hence more deposition was possible in the middle and at the end of the preform. Furthermore, the amount of deposition at the end is more than that in the middle of the preform because of the accumulated reactant gas at the exit. Even though the experimental data do not fit to the numerical calculation results because of the different structure of the reactor, they indicate the reasonableness of the operational parameter values.

CONCLUSIONS

Mathematical modeling of the chemical vapor infiltration of SiC into the fabric preform in the isothermal forced flow reactor with a gas mixture of reactant MTS and hydrogen was studied. When the reaction time is 130 min, pore entrances are plugged. At the time of plugging pores, the pressure at the gas entrance increases sharply. There remains a non-uniform deposition through the whole preform at the time of plugging pores. When pores at the gas entrance are plugged, the fractions of MTS and HCl at the gas exit approach 0 and 0.42, respectively.

The time when the preform should be overturned in the middle of the process could be decided by observing the time changes of fiber radius at the gas entrance.

ACKNOWLEDGMENT

Authors are grateful for the financial support from the Agency for Defense Development (ADD).

NOMENCLATURE

A : cross sectional area of the preform
C : concentration of gas [mol/cm^3]
d_f : diameter of a fiber [cm]
H : height of the preform [cm]
k : deposition rate constant per unit lateral surface area of a fiber [cm/min]
M_m : molecular weight of deposited SiC [g/mol]
N : number of fibers in a bundle
n : stoichiometric coefficient
P : pressure [torr]
Q : volumetric flow rate of gas [cm/min]
q : number of deposited SiC molecule per molecule of reactant MTS
r_f : radius of a fiber [cm]
t : time [min]
W : number of filaments per unit cross-sectional area perpendicular to the axis of filaments [cm^{-2}]
z : distance along the direction of gas flow [cm]

Greek Letters

ε : local porosity of a ply
μ : viscosity of gas [g/cm s]
ρ : density of gas [g/cm^3]
ρ_m : density of the deposited SiC [g/cm^3]
σ : dimensionless radius of a fiber; r_f/r_{fo}
ξ : dimensionless distance in z-direction; z/H

Subscripts

A : MTS
i : i-component
f : fiber
o : zero time
z : at z

REFERENCES

Bickerdike, R. J., Brown, A. R. G., Hughes, G. and Ranson, H., in the Proceedings of the Fifth Conference on Carbon, 1 (1992).

Birakayala, N. and Evans, E. A., "A Reduced Reaction Model for Carbon CVD/CVI Processes," *Carbon*, **40**(5), 675 (2002).

Bird, R. B., Stewart, W. E. and Lightfoot, E. N., "Transport Phenomena," 2nd ed., John Wiley & Sons, Inc., New York, 191 (2002).

Cho, M. S., Kim, J. W. and Chung, G. Y., "Manufacturing of Ceramic Composites Reinforced with Layered Woven Fabrics by CVI of SiC from Dichlorodimethylsilane," *Korean J. Chem. Eng.*, **13**, 515 (1996).

Chung, G. Y., McCoy, B. J., Smith, J. M., Cagliostro, D. E. and Carswell, M., "Chemical Vapor Infiltration: Modeling Solid Matrix De-

position in Ceramic-Ceramic Composites," *Chem. Eng. Sci*., **46**(3), 723 (1991).

Chung, G. Y. and McCoy, B. J., "Modelling of CVI for Ceramic Composites Reinforced with Layered Woven Fabrics," *J. Am. Ceram. Soc*., **74**(4), 746 (1991).

Chung, G. Y., Cagliostro, D. E., McCoy, B. J. and Smith, J. M., "Rate of Chemical Vapor Deposition of SiC and Si on Single Layer Woven Fabrics," *NASA T.M*., 10397 (1992).

Chung, G. Y., McCoy, B. J., Smith, J. M. and Cagliostro, D. E., "Chemical Vapor Infiltration: Modeling Solid Matrix Deposition for Ceramic Composites Reinforced with Layered Woven Fabrics," *Chem. Eng. Sci*., **47**(2), 311 (1992).

Chung, G. Y., McCoy, B. J., Smith, J. M. and Cagliostro, D. E., "Chemical Vapor Infiltration: Dispersed and Graded Depositions for Ceramic Composites," *AIChE J*., **39**(11), 1834 (1993).

Delhaes, P., "Chemical Vapor Deposition and Infiltration Processes of Carbon Materials," *Carbon*, **40**(5), 641 (2002).

Jenkin, W. C., *U.S. Patent*, 3,160, 517 (1964).

Jensen, K. F. and Melkote, R. R., "Chemical Vapor Infiltration of Short Fiber Preforms," Extended Abstract presented at the 1989 AIChE Meeting, San Francisco, 54 (1989).

Jiang, K., Li, H. and Wang, M., "The Numerical Simulation of Thermal-Gradient CVI Process on Positive Pressure Condition," *Materials Letters*, **54**, 419 (2002).

Jin, S., Wang, X. and Starr, T. L., "A Model for Front Evolution with a Non-local Growth Route," *J. Mater. Res*., **14**, 3829 (1999).

Jin, S., Wang, X., Starr, T. L. and Chen, X., "Robust Numerical Simulation of Porosity Evolution in Chemical Vapor Infiltration I: Two Space Dimension," *J. Computational Physics*, **162**(2), 467 (2000).

Gupte, S. M. and Tsamopoulos, J. A., "Densification of Porous Material by Chemical Vapor Infiltration," *J. Electrochem. Soc*., **136**, 555 (1989).

Kim, J. W., Cho, M. S. and Chung, G. Y., "Manufacturing of Ceramic Composites Reinforced with Carbon Fibers through CVI," *Korean Chem. Eng. Res*., **34**, 443 (1996).

Lee, S. J., Kim, M. H., Kim, Y. T. and Chung, G. Y., "Studies on the Preparation of C/SiC Composites as a Catalyst Support by CVI in a Fluidized Bed Reactor," *Korean J. Chem. Eng*., **19**, 167 (2002).

Li, H. J., Jiang, K. Y. and Li, K. Z., "Optimizing Parameters of CVI Processes for Manufacturing Carbon-Carbon Composites by Genetic Algorithms," *Materials Letters*, **57**, 2366 (2003).

Luo, R., "Fabrication of Carbon/Carbon Composites by an Electrified Preform Heating CVI Method," *Carbon*, **40**(11), 1957 (2002).

Nannetti, C. A., Riccardi, B., Ortona, A., La Barbera, A., Scafe, E. and Vekinis, G., "Development of 2D and 3D Hi-Nicalon Fibers/SiC Matrix Composites Manufactured by a Combined CVI-PIP Route," *Nuclear Materials*, **307-311**, 1196 (2002).

Park, J. Y., Kim, W. J. and Hwang, H. S., "Studies on the densification of C_f/SiC composites using MTS," The 1st year Technical Report, The Korea Nuclear Research Center (2001).

Rossignol, J. Y., Langlais, F. and Naslain, R., "A Tentative Modelization of Titanium Carbide CVI within the Pore Network of Two Dimensional Carbon-Carbon Composite Preforms," *Proc. Electrochem. Soc*., **84**(6), 596 (1984).

Starr, T. L., "Model for CVI of Short Fiber Preforms," *Ceram. Eng. Sci. Proc*., **8**(7), 951 (1987).

Tai, N. H. and Chou, T. W., "Analytical Modeling of Chemical Vapor Infiltration of Ceramic Composites," *J. Amer. Ceram. Soc*., **72**(3), 414 (1989).

Zhang, W. and Hüttinger, K. J., "Simulation Studies on CVI of Carbon," *Composites Science and Technology*, **62**(15), 1947 (2002).